Protective effect of L-carnitine against oxidative stress injury in human ovarian granulosa cells

XUENING LI[1*], XIAODONG WU[1*], TIANYI MA[2*], YUEMIN ZHANG[3], PINGPING SUN[3], DANDAN QI[3] and HUAGANG MA[3]

[1]School of Clinical Medicine, Weifang Medical University, Weifang, Shandong 261000, P.R. China;
[2]Faculty of Engineering and IT, University of Technology Sydney, Sydney, New South Wales 2007, Australia;
[3]Center of Reproductive Medicine, Weifang People's Hospital, Weifang, Shandong 261000, P.R. China

Received April 25, 2022; Accepted October 31, 2022

DOI: 10.3892/etm.2023.11860

Abstract. Granulosa cells (GCs) are important for supporting and nourishing oocytes during follicular development and maturation. Oxidative stress (OS) injury of GCs can lead to decreased responsiveness of follicles to follicular stimulating hormone (FSH), which will accelerate ovarian senescence and adversely affect oocyte and embryo quality. Since L-carnitine has been previously reported to exert strong antioxidant activity, the present study aimed to explore the possible effects of L-carnitine on OS injury and FSH receptor (FSHR) expression in ovarian GCs, results of which may be of significance for GCs protection. In the present study, OS was induced *in vitro* in KGN cells by treatment with H_2O_2. KGN cells were cultured and divided into the following four groups: Blank, OS, and 40 and 80 μmol/l L-carnitine pre-treatment groups. In the OS group, cells showed nuclear pyknosis, mitochondria swelled irregularly whilst featuring fractured cristae. In addition, cell viability, ROS levels, superoxide dismutase levels, glutathione levels, malondialdehyde levels, the mitochondrial membrane potential and FSHR expression, as determined by Cell Counting Kit-8 (CCK-8), 2,7-dichloro-dihydrofluorescein diacetate, spectrophotometry, ELISA, spectrophotometry, JC-1 and western blot analyses, respectively, were all significantly different in the OS group compared with those in the control group. However, malonaldehyde levels, reactive oxygen species levels and the apoptosis rate according to flow cytometry were all significantly increased compared with those in the control. Compared with those in the OS group, the morphology of cells and mitochondria in the L-carnitine pre-treatment groups were improved, whilst cell viability and the expression of FSHR were significantly increased but oxidative stress injury was decreased. The present results suggest that L-carnitine can protect the cells from OS damage induced by H_2O_2, enhance antioxidant activity whilst suppressing the apoptosis of GCs, in addition to preserving FSHR expression in GCs under OS. Therefore, the present study revealed that the introduction of L-carnitine in clinical medicine or dietary supplement may protect GCs, improve follicular quality and female reproductive function.

Correspondence to: Dr Huagang Ma, Center of Reproductive Medicine, Weifang People's Hospital, 151 Guangwen Street, Kuiwen, Weifang, Shandong 261000, P.R. China
E-mail: mahuagang@126.com

[*]Contributed equally

Key words: L-carnitine, ovarian granulosa cells, oxidative stress, follicular stimulating hormone receptor, mitochondria

Introduction

Forming part of the basic unit of female reproduction, a follicle consists of oocyte and granulosa cells (GCs) (1). GCs are involved in supporting and nourishing oocytes during follicular development and maturation (2,3). Oxidative stress (OS) caused by the increase of reactive oxygen species (ROS) levels has an important effect on oocyte and embryo quality (4,5). Previous study have found that the levels of ROS in the follicular fluid of patients with polycystic ovary syndrome (PCOS) and endometriosis (EMT) are significantly increased (4,6). In addition, within the healthy population, the total oxidative state and total antioxidant state in the follicular fluid also tend to be abnormal as the individual ages (6-8). Other studies have confirmed that OS can reduce the ovarian follicle stimulating hormone (FSH) activity by downregulating the expression of the FSH regulatory gene P450 aromatase and then decreasing the expression of FSHR (9,10). Therefore, it is important to protect GC from OS injury to improve the quality of follicles and embryos, in addition to preserving female reproductive function.

L-carnitine (LC) is a type of water soluble vitamin analogue that is naturally occurring in the human body (11). As an important substance of aliphatic acid energy metabolism, it can help transport long chain aliphatic acids from the cytoplasm into the mitochondria (12). Since L-carnitine is a carrier of long-chain fatty acyl groups, it can participate in the deacylation and reacylation of membrane phospholipids in the process of membrane repair, which is conducive to timely membrane repair (12). In other words, LC exhibits high antioxidant effects. Although previous studies have demonstrated

that LC exerts protective effects on female reproduction by reducing the damage of oocytes by oxidative stress products (such as ROS) by reducing oocyte oxidative stress, which improves oocyte quality (13,14), the potential role of LC in GCs remains unclear. Therefore, the present study firstly introduced LC into an *in vitro* model of OS in GCs, which is established in the ovarian granular cell line KGN through H_2O_2 treatment. OS biomarkers and FSH receptor (FSHR) protein expression levels were then measured to explore the effects of LC on OS injury in KGN cells induced by H_2O_2. The present study examined the morphological changes of KGN cells in the aforementioned groups using electron microscopy, measured the levels of oxidative stress [2,7-dichloro-dihydrofluorescein diacetate (DCFH-DA) assay of ROS, spectrophotometry of superoxide dismutase levels, ELISA of glutathione levels, spectrophotometry of malondialdehyde (MDA) levels], and examined cell apoptosis using flow cytometry and FSHR expression using western blotting to explore the effects of LC on the response of KGN cells to oxidative stress.

Materials and methods

Reagents. LC (purity >98%) was purchased from Sigma-Aldrich (Merck KGaA). H_2O_2 30% solution (analytical grade) was purchased from Yantai Far East Fine Chemical Co., Ltd. KGN human ovarian granulocyte cells (cat. no. YS549C) were purchased from Shanghai Yaji Biotechnology Co., Ltd. The KGN cells were authenticated by short tandem repeat profiling.

Culture of KGN cells. KGN cells are anchorage-dependent cells and can proliferate steadily (15). KGN cells maintain the majority of the physiological activities of normal human ovarian GCs, including functional FSHR expression, steroid production and Fas-mediated apoptotic patterns (16). They are suitable for studying the physiological regulation of human GCs (16). KGN cells were cultured in complete medium (CM), which was comprised of 89% DMEM/F-12 (Beijing Oka Biological Technology Co., Ltd.), 10% FBS (ExCell Biotechnology Co., Ltd.) supplement and 1% penicillin (100 U/ml) and streptomycin (0.1 mg/ml) (Beijing Biosharp Biotechnology Co., Ltd.) at 37˚C with 5% CO_2. The cells able to multiply normally were cryopreserved once every other week with 1 ml cryoprotectant made of DMSO (Beijing Solarbio Science & Technology Co., Ltd.) and FBS at a ratio of 1:9.

KGN cells were divided into the following groups for the Cell Counting Kit-8 (CCK-8), OS level (DCFH-DA, spectrophotometry, ELISA and spectrophotometry), JC-1 and western blotting assays: Blank (CM-blank 24 h + CM-blank 24 h), OS (CM-blank 24 h + CM-H_2O_2 100 μmol/l 24 h), low LC (CM-LC 40 μmol/l 24 h + CM-H_2O_2 100 μmol/l 24 h) and high LC (CM-LC 80 μmol/l 24 h + CM-H_2O_2 100 μmol/l 24 h) groups.

Determination of H_2O_2 concentration needed to induce OS. KGN cells ($1x10^3$ cells/well) were seeded into a 96-well plate and cultured at 37˚C for 24 h. Cells were then divided into the following groups: Control (cells without H_2O_2 treatment); treatment (cells treated with 25, 50, 100, 150 and 200 μmol/l H_2O_2) and the blank groups (wells without cells or H_2O_2 treatment). After culture for 12, 24 and 48 h at 37˚C, 10 μl CCK-8 solution (Beijing Solarbio Science & Technology Co., Ltd.) was added to each well according to the manufacturer's protocols. The plates were incubated for 2 h at 37˚C and the absorbance at 450 nm wavelength, which was obtained as the optical density (OD) value, was measured with a Multiskan SkyHigh automatic microplate reader (Thermo Fisher Scientific, Inc.). Cell viability was calculated using the following formula: Cell viability=$(OD_{treatment}-OD_{blank})/(OD_{control}-OD_{blank})$ x100. The appropriate concentration of H_2O_2 in CM was screened out by monitoring changes in cell viability and cell viability of 50-60% was selected to construct the OS model for subsequent experiments. Cell viability was assessed in three replicates for each group.

Determination of the concentration of LC. KGN cells had a relatively long population doubling time of ~46.4 h (13), therefore, the cells were sub-cultured at a 1:2 ratio. Subsequently, cells were cultured in CM containing 80 μmol/l LC for 24 h and then the CM containing 100 μmol/l H_2O_2 was replaced to culture cells for a further 24 h at 37˚C. The duration of 24 h was selected because a culture time of two times 24 h was close to its doubling time (15).

Effect of LC concentration on KGN cell viability. KGN cells ($5x10^3$ cells/well) were seeded into a 96-well plate and divided into the control group (cells without LC treatment) and the experimental groups (cells treated with 10, 20, 40, 80 and 160 μmol/l LC at 37˚C). The OD data were corrected for the OD of the blank group (wells without cell or LC treatment) and then normalized to the control group. After 24 h, cell viability was calculated according to the manufacturer's instructions using CCK-8 (cat. no. BS350A; Biosharp Life Sciences) at 37˚C for 4 h. This cell viability experiment was assessed in three replicates for each group.

LC concentration in KGN cells. KGN cells ($1x10^5$ cells/well) were seeded into a six-well plate without the blank group. Aliquots of 2 ml CM containing different LC concentrations (10, 20, 40, 80 and 160 μmol/l LC at 37˚C) were added to each well and before intracellular LC concentrations were detected after 24 h at 37˚C. After washing with PBS, cells were digested with 1 ml trypsin (cat. no. T1300, Beijing Solarbio Science & Technology Co., Ltd.) for 1 min and collected in a 1.5-ml Eppendorf tube. After further washing with PBS, cells were resuspended in 1 ml PBS, repeatedly frozen and thawed (-80˚C and 37˚C) for three times. Subsequently, cells were centrifuged at 590 x g for 20 min and the LC concentration in the supernatant was measured using ELISA (cat. no. ml037170; Shanghai Enzyme-linked Biotechnology Co., Ltd.) according to the manufacturer's protocols. Sample concentrations were extrapolated from a calibration curve. Sample concentrations were tested three times. The concentration of LC was selected according to the change in LC concentration in GCs under different extracellular concentrations of LC.

Observation of the ultrastructure of KNG cells. Cells were cultured to $1x10^7$ cells in each group: Blank (CM-blank 24 h + CM-blank 24 h), OS (CM-blank 24 h + CM-H_2O_2 100 μmol/l 24 h), low LC (CM-LC 40 μmol/l 24 h + CM-H_2O_2 100 μmol/l 24 h) and high LC (CM-LC 80 μmol/l 24 h + CM-H_2O_2 100 μmol/l 24 h) groups. After digestion at 37˚C

with 1 ml trypsin for 1 min, the cells were collected in a 1.5-ml Eppendorf tube and centrifuged at 100 g for 10 min to remove the supernatant. Subsequently, cells were fixed in 4% paraformaldehyde + 1% glutaraldehyde solution for 30 min at 37˚C and stored at 5˚C for 12 h. After removal of the fixative solution, cells were rinsed with PBS three times for 15 min each time. Subsequently, cells were fixed with 1% osmium tetroxide solution for 1-2 h at 37˚C, washed with PBS, dehydrated in ascending ethanol series (30, 50, 70, 80, 90 and 95% ethanol; 15 min each) before being finally treated with 100% ethanol for 20 min. After treatment with pure acetone for 20 min, the cells were treated with a mixture of embedding agent and acetone (V/V=1/1 for 1 h, then V/V=3/1 for 3 h) and pure embedding agent overnight. The osmotic samples were heated overnight at 70˚C. The samples were sliced into 70-90-nm sections using an ultrathin slicing machine (HT7700; Hitachi, Ltd.) and stained with lead citric acid solution and 50% ethanol saturated solution of uranium dioxane acetate for 5-10 min, respectively. After exposure to air, the specimens were observed under transmission electron microscopy (EM UC7; Leica Microsystems GmbH) to analyze the morphology of the nuclear membranes and mitochondria. The specific method was consistent with that used by Ma *et al* (17).

Measurement of cell viability and OS levels

Cell viability. A total of $1x10^6$ KGN cells were cultured in a 96-well plate at 37˚C as follows: Blank group (CM-blank 24 h + CM-blank 24 h), OS (CM-blank 24 h + CM-H_2O_2 100 μmol/l 24 h), low LC (CM-LC 40 μmol/l 24 h + CM-H_2O_2 100 μmol/l 24 h) and high LC groups (CM-LC 80 μmol/l 24 h + CM-H_2O_2 100 μmol/l 24 h). Subsequently, cell viability of each experimental group was detected using CCK-8 assay.

OS levels. A total of $1x10^6$ KGN cells were cultured in a 96-well plate at 37˚C: Blank group (CM-blank 24 h + CM-blank 24 h), OS (CM-blank 24 h + CM-H_2O_2 100 μmol/l 24 h), low LC (CM-LC 40 μmol/l 24 h + CM-H_2O_2 100 μmol/l 24 h) and high LC groups (CM-LC 80 μmol/l 24 h + CM-H_2O_2 100 μmol/l 24 h). ROS (cat. no. CA1410), MDA content (cat. no. BC0020), reduced glutathione (GSH) content (cat. no. BC1175) and superoxide dismutase (SOD) activity (cat. no. BC0170) assay kits, all purchased from Beijing Solarbio Science & Technology Co., Ltd., were used to analyze the OS levels *in vitro*, according to the manufacturer's protocols.

ROS. The ROS level in KGN cells was measured based on the fluorescence intensity of DCFH-DA. After washing with PBS, cells were treated with 1 ml working solution (DCFH-DA: serum-free medium=1:1,000). ROS detection solution was prepared with the DCFH-DA probe in serum-free medium at 1:1,000 ratio and 1 ml ROS detection solution was added into the six-well plate to cover the bottom of the wells. After cultured for 25 min at 37˚C, the cells were gently washed with DMEM and digested with 500 μl trypsin without EDTA for 3 min at 37˚C. The average fluorescence intensity of KGN cells in each experimental group was recorded using the fluorescein isothiocyanate (FITC) channel of a NovoCyte 2040R flow cytometer (Beckman Coulter, Inc.) and analyzed using NovoExpress 1.1.0 (Agilent Technologies, Inc.) within 1 h. The maximum absorption and excitation wavelengths of FITC were 494 and 518 nm, respectively. The ROS level analysis was performed in triplicate.

MDA. KGN cells in the Blank (CM-blank 24 h + CM-blank 24 h), OS (CM-blank 24 h + CM-H_2O_2 100 μmol/l 24 h), low LC (CM-LC 40 μmol/l 24 h + CM-H_2O_2 100 μmol/l 24 h) and high LC (CM-LC 80 μmol/l 24 h + CM-H_2O_2 100 μmol/l 24 h) groups were washed with PBS, digested with 400 μl trypsin for 1 min at 37˚C and resuspended in an Eppendorf tube. A total of 10 μl cell suspension was collected for cell counting using a hemocytometer. After cell counting, the cells in each group were centrifuged at 210 x g for 5 min at 37˚C to remove the supernatant and then diluted in PBS to $5x10^6$ cells/ml. Cell disruption was performed at 4˚C using an ultrasonic breaker (KQ-800GKDV; Kunshan Ultrasonic Instrument Co., Ltd.) for 30 cycles of sonication at 20% power for 3 sec with an interval of 10 sec between each sonication. Subsequently, the broken cells were centrifuged at 8,000 g and 4˚C for 10 min to collect the supernatant that was stored at 4˚C until further use. The samples were treated with the MDA content assay kit as per manufacturer's protocols and sealed in water bath at 100˚C for 60 min. After cooling to room temperature (~1 h), the samples were centrifuged at 10,000 g and room temperature for 10 min, before 200 μl were added into each well of a 96-well plate. The absorbance at 450, 532 and 600 nm in each well was determined and ΔOD was obtained as the OD difference between test well and blank well at the same wavelength. MDA content in each sample was calculated using the following formula: MDA content=$[12.9x (\Delta OD_{532}-\Delta OD_{600})-2.58x \Delta OD_{450}] x V_{total}/(500/V_{extract} x V_{sample})$. The MDA content was measured three times.

GSH. KGN cells in a six-well plate were collected and counted to ensure a number of cells of $1x10^6$-$1x10^7$. After centrifugation at 600 x g and 10 min at room temperature, cells were washed twice with PBS and then treated with the working solution according to the manufacturer's protocol of the specific kit. After being frozen (30 min) and thawed (30 min) for three times, the samples were centrifuged at 8,000 x g for 10 min at room temperature and the supernatants were collected and stored at 4˚C until further analysis. A calibration curve was prepared according to the manufacturer's protocols of the specific kit and the sample supernatants were loaded into a microplate reader. For each sample, the absorbance at 412 nm was measured and the detection absorbance of the blank detection hole was set as D_0. $\Delta OD_{412}=OD_{412}-OD_0$). Subsequently, the calibration curve was used to extrapolate the concentration of each sample from the corresponding ΔOD_{412}. The GSH content was calculated using the following formula: Sample concentration x $V_{sample}/(V_{sample}/V_{sample\ total}$ x cell number), i.e. the ratio between sample concentration and cell number. The GSH content was measured three times.

SOD. The protocol used to measure the SOD content was the same as that for MDA in terms of experimental groups and treatments, cell counting and disruption, as well as supernatant collection. The SOD activity detection kit was purchased from Beijing Solarbio Science & Technology Co., Ltd. (product no. BC0170). The supernatants collected from each sample were loaded in the microplate reader according to the kit protocols before the test, control (untreated KGN cells) and blank (no cells) samples were set. After sample loading using the loading buffer in the kit to prevent excessive protein degradation, the supernatants and the assay reagents in each tube were mixed, incubated at 37˚C for 30 min and cooled down to

room temperature. Samples were added into 96-well plate at the volume of 200 μl per well and the absorbance at 560 nm of each sample was measured using a microplate reader. ΔOD_{test} was the difference of OD_{test} and $OD_{control}$, whereas ΔOD_{blank} was the difference of OD_{blank1} and OD_{blank2} (blank1 and blank2 were replicates. This step aimed to eliminate systematic errors). The inhibition percentage was calculated using the following formula: % Inhibition=(ΔOD_{blank}-ΔOD_{test})/ΔOD_{blank} x100. The cell number of samples were adjusted to 1.2 x10^6 to ensure the inhibition percentage of 30-70% based on preliminary experiments. Therefore, the SOD activity was calculated using the following formula: SOD activity=inhibition percentage x $V_{reaction}$/(1-inhibition percentage)/(500/$V_{sample\ total}$ x V_{sample}) x Dilution ratio. The SOD content was measured three times.

Measurement of mitochondrial membrane potential (ΔΨm) and cell apoptosis

ΔΨm. The ΔΨm was measured using the Mitochondrial Membrane Potential Detection Kit (JC-1 Assay; cat. no. CA1310; Beijing Solarbio Science & Technology Co., Ltd.) according to the manufacturer's protocols. Cells were cultured in six-well plates and 4 ml 200X JC-1 dye solution diluted with ultrapure water at a ratio 1:160 was added with 1 ml 5X JC-1 dyeing buffer solution to prepare the JC-1dyeing working solution. After washing with PBS, the cells were treated with 1 ml CM-blank or JC-1 dyeing working solution and incubated at 37˚C for 20 min. The distilled water and 5X JC-1 dyeing buffer were mixed in a 4:1 ratio to obtain 1X JC-1 dyeing buffer. After incubation, cells were gently washed two times with the 1X JC-1 dyeing buffer and 2 ml CM-blank was added into each well. The samples were observed under a fluorescence microscope (magnifications, x200 and s400; IX73 DP22; Olympus Corporation) within 1 h. The JC-1 monomers diluted in the cytoplasm of KGN cells were excited using blue light to present green fluorescence, whilst the JC-1 aggregates in the mitochondrial matrix of KGN cells were excited using green light to present red fluorescence. The maximum excitation and emission wavelengths of JC-1 monomer (green light) are 514 and 529 nm respectively. The maximum excitation wavelength of the JC-1 polymer (J-aggregates; red light) is 585 nm, and the maximum emission wavelength is 590 nm. The presence of green fluorescence in the cytoplasm indicates a decrease in mitochondrial membrane potential, where the cells would be considered in the early stages of apoptosis, whilst red fluorescence would indicate normal mitochondrial membrane potential and the cells are likely to be in normal condition. The images displaying either green or red fluorescence were merged using the ImageJ V1.8.0 software (National Institutes of Health). The ΔΨm measurement was performed three times and calculated according to the kit instructions.

Cell apoptosis. Cell apoptosis was detected using a ACEA NovoCyte flow cytometer (ACEA Bioscience, Inc.) according to the protocols of the Annexin V-FITC/PI double-staining kit (cat. no. 40302ES20; Shanghai Yeasen Biotechnology Co., Ltd.). KNG cells were digested with 400 μl trypsin and collected by centrifugation at 300 g and 4˚C for 5 min. A total of 1x10^6 Cells were washed twice with cold PBS and resuspended with 100 μl 1X Binding Buffer, before they were gently mixed with Annexin V-FITC (5 μl) and PI staining solution (10 μl). The control was only composed of Annexin V-FITC and PI staining solution without cells. The cells were stored away from light to react at room temperature for 15 min, mixed with 400 μl 1X binding buffer and stored on ice. Samples were analyzed within 1 h and FITC and PI channels were selected. The results were graphically analyzed using the Novoexpress 1.5.6 software (Agilent Technologies, Inc.). The experiment was performed three times.

Detection of FSHR protein expression in GCs. Total protein was extracted from KNG cells using 500 μl RIPA lysis buffer (RIPA and PMSF at a ratio of 100:1). RIPA (product no. R0010) and PMSF (product no. P0100) were purchased from Beijing Solarbio Science & Technology Co., Ltd. After lysis on ice in the dark for 30 min, the cells were scraped and transferred into an Eppendorf tube for centrifugation at 13,680 x g and 4˚C. The supernatants were collected and total protein contents were measured using a BCA protein quantitative detection kit. RIPA was used to adjust the total protein concentration of supernatants in each group to the same value and 5X protein loading buffer was added according to the samples in a 5:1 ratio. The protein samples were boiled at 100˚C for 5 min and the 10% polyacrylamide gel was prepared using a PAGE Gel rapid preparation kit. Protein (30 μg per lane) separation was performed by SDS-PAGE using the voltage of 80 V for 30 min and 120 V for 1 h, before the proteins were transferred onto PDVF membranes. After washing three times with TBST (0.5% Tween; cat. no. T1085; Beijing Solarbio Science & Technology Co., Ltd.), the samples were blocked with 5% milk for 2 h at 37˚C and incubated with primary antibodies against FSHR (1:1,500; cat. no. 22665-1-AP; ProteinTech Group, Inc.) and GAPDH (1:10,000, cat. no. 60004-1-Ig; ProteinTech Group, Inc.) overnight at 4˚C, then incubated with the HRP-IgG secondary antibodies (1:10,000, cat. no. PR30011; ProteinTech Group, Inc.) for 1 h at 37˚C. Subsequently, the membranes were washed and the protein bands were developed using Omni-ECL™ basic chemiluminescence detection Kit (cat. no. SQ201; Shanghai Epizyme Biotech Co., Ltd.). Luminescence imaging was performed using a chemiluminescence imager (ChemiDoc touch; Bio-Rad Laboratories, Inc.). The experiment was repeated three times. ImageJ V1.8.0 software was used to quantify protein expression.

Statistical analysis. SPSS 25.0 (IBM Corp.) and GraphPad Prism 8.0 (GraphPad Software, Inc.) were used for statistical analysis. Data are expressed as the mean ± standard deviation. Levene's test was used to test the homogeneity of variance in each group. If the variance was homogeneous, Tukey's test would be used. By contrast, if the variance was not homogeneous, then Welch ANOVA and Dunnett's T3 test would be used. All experiments were repeated ≥ three times and $P<0.05$ was considered to indicate a statistically significant difference.

Results

Determination of the H_2O_2 concentration needed to induce OS. KGN cells were cultured at different H_2O_2 concentrations (0, 25, 50, 100, 150 and 200 μmol/l) and cell viability was measured through CCK-8 assay at different timepoints after treatment with H_2O_2 (12, 24 and 48 h). Cell viability of each group decreased as the H_2O_2 concentration increased

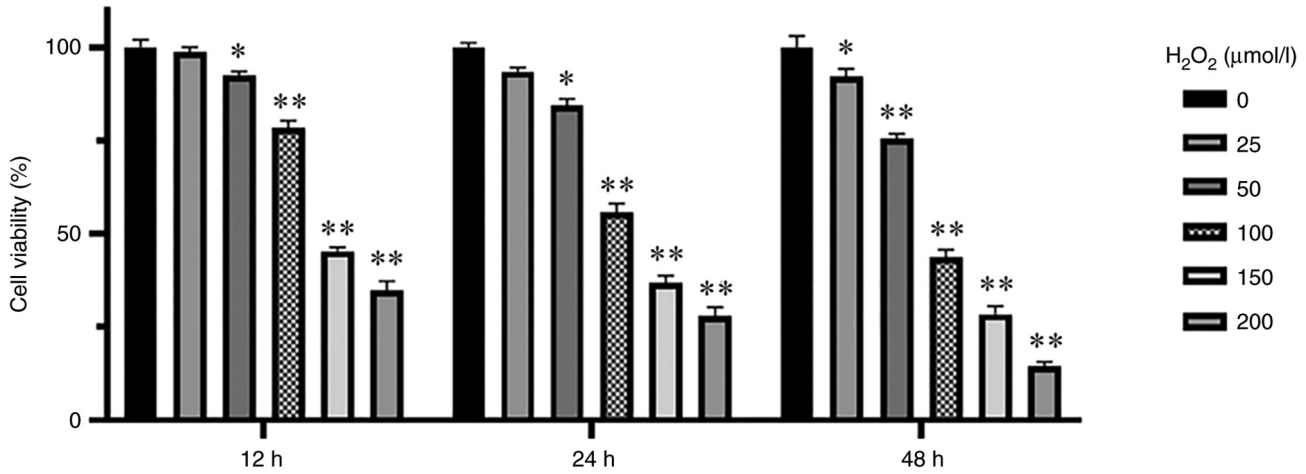

Figure 1. Cell viability is decreased in KGN cells challenged with H_2O_2. Effect of several H_2O_2 treatment concentrations and durations on the cell viability of KGN cells. *P<0.05 and **P<0.01 vs. control (untreated cells), Tukey's test. Data are represented as the mean ± standard deviation (n=3).

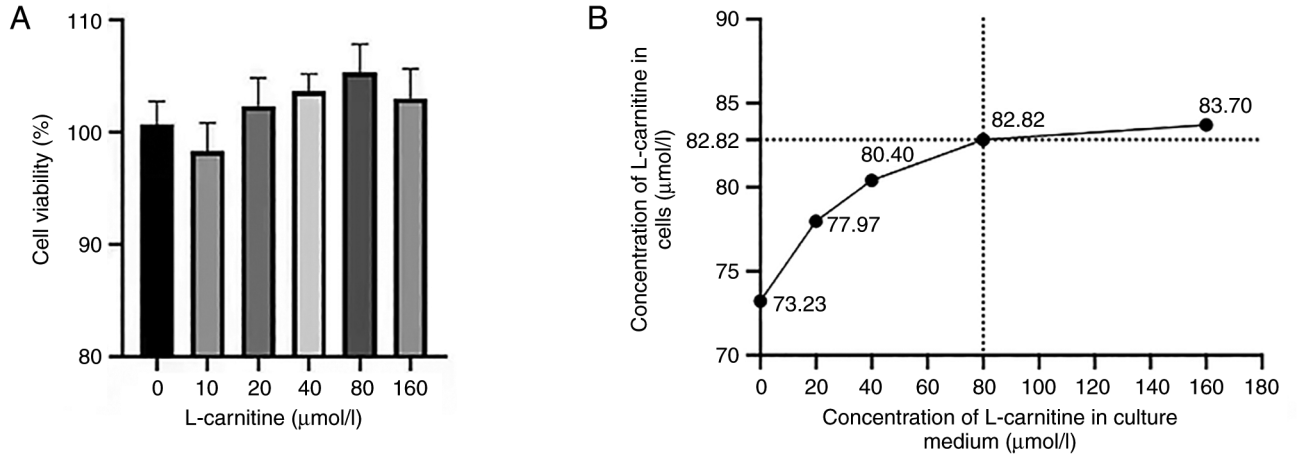

Figure 2. L-carnitine concentration. (A) Effects of different concentrations of L-carnitine on the viability of KGN cells. (B) Analysis of the intracellular concentrations of L-carnitine after exposure to different concentrations of L-carnitine. Data are represented as the mean ± standard deviation (n=3).

compared with that in the control group, reaching significance at H_2O_2 concentrations of >50 μmol/l for 24 h (P<0.05; Fig. 1). Therefore, 100 μmol/l H_2O_2 were used to treat KGN cells for 24 h to induce OS in the KGN cells.

Determination of the optimal LC concentration. LC exerted no significant effects on cell viability (Fig. 2A). ELISA showed that increasing the LC concentration from 80 to 160 μmol/l did not result in a significant increase in the concentration of LC internalized by the cells, whilst cell viability was decreased slightly (Fig. 2B). Therefore, 80 μmol/l LC was chosen for further experiments, and 40 μmol/l was used as a median control.

Effect of LC pretreatment on cell viability in the presence of H_2O_2-induced OS. Compared with that in the control group, the cell viability in the H_2O_2-only group was significantly decreased (P<0.01; Fig. 3). Compared with that in the H_2O_2-only group, the cell viability of all LC pre-treated groups were all significantly increased in a dose-dependent manner (P<0.01; Fig. 3).

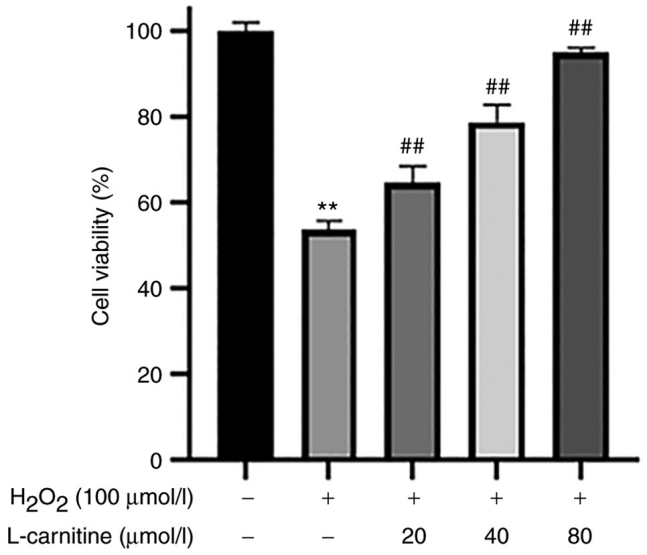

Figure 3. Effects of L-carnitine pre-treatment on the viability of KGN cells challenged with H_2O_2. **P<0.01 vs. control and ##P<0.01 vs. H_2O_2-only, Tukey's test. Data are represented as the mean ± standard deviation (n=3).

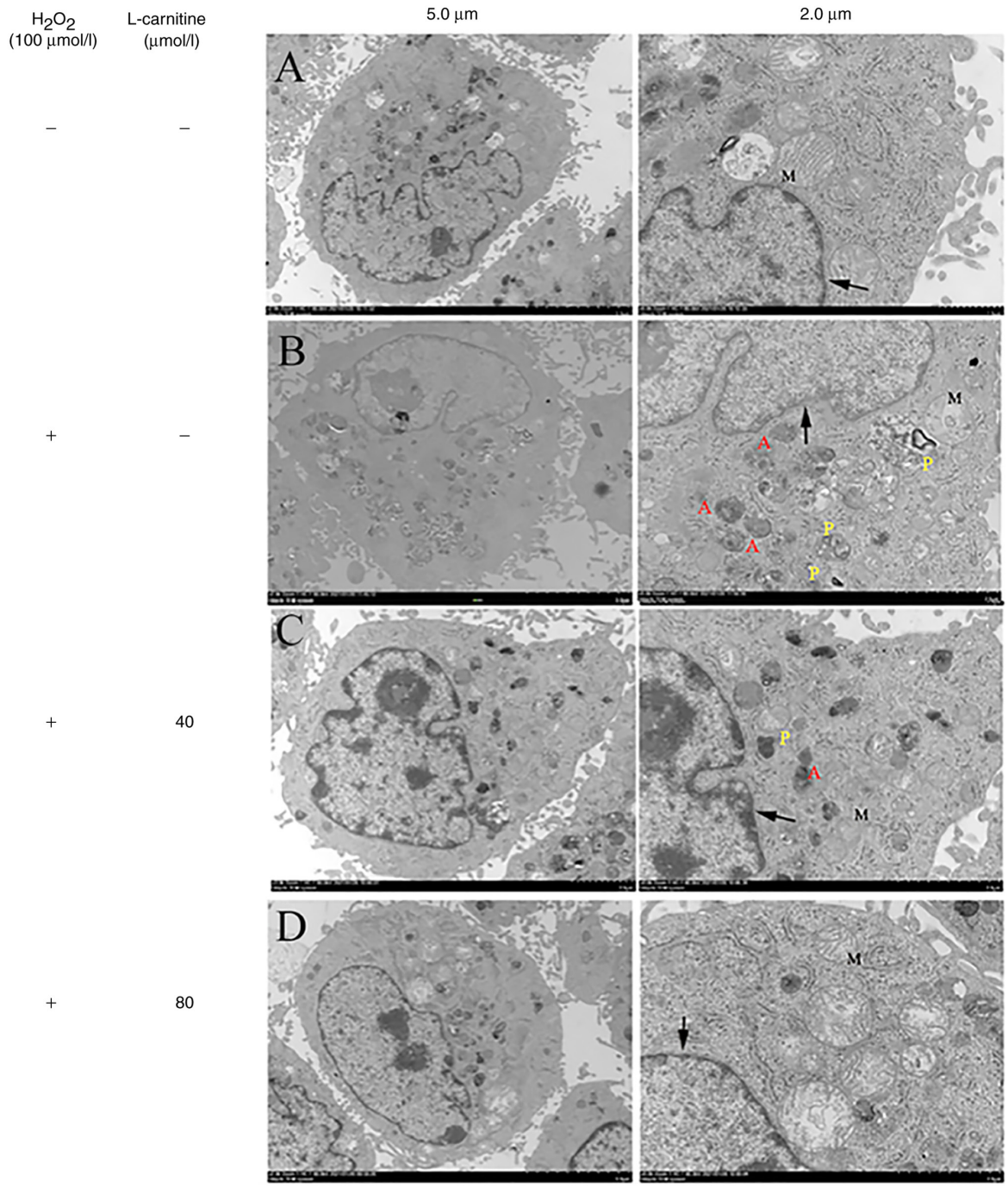

Figure 4. Ultrastructure of untreated KGN cells, those treated with H_2O_2 and those pre-treated with L-carnitine as analyzed using transmission electron microscopy. The arrows indicate the nuclear membrane. (A) In the control group, the nucleus is complete, the nuclear membrane is clear, the mitochondrial structure is complete and the mitochondrial ridge is clearly visible. (B) In the H_2O_2-only group, the nucleolus is diffused, the nuclear membrane is blurred, the nuclear membrane in some areas disappeared. The majority of mitochondria do not present with the complete structure and there is a large number of apoptotic and phagocytic bodies in the cytoplasm. (C) In the low L-carnitine group (40 μmol/l), the nucleus is heterogeneous, the nuclear membrane in some areas is fuzzy, some mitochondria were visible, the structure in the mitochondria is unclear and apoptotic. Phagocytic bodies are visible in the cytoplasm. (D) In the high L-carnitine group (80 μmol/l), the nucleus is complete, the nuclear membrane is basically clear, the mitochondrial structure is basically complete and a clear mitochondrial ridge can be seen. Magnifications: Left, x2,000; right, x5,000. M, mitochondria; P, phagosome; A, apoptotic body.

Ultrastructure of KGN cells. KGN cells in the control group showed intact nucleolus, clear nuclear membrane and normal mitochondrial morphology, whilst in the H_2O_2-only group and the 40 and 80 μmol/l LC pretreatment groups, different degrees of early and late apoptosis appeared in electron microscopy (Fig. 4). In the blank control group, the cells showed a spindle-shaped extension state under the light microscope and were well attached to the wall. Under the electron microscope, it was observed that the cell structure was complete, the nucleolus was complete, the nuclear membrane was clear, the mitochondrial morphology and structure were normal, and the mitochondrial crest was clearly visible. In the injury model group, the density of KGN cells decreased, floating dead cells and cell debris

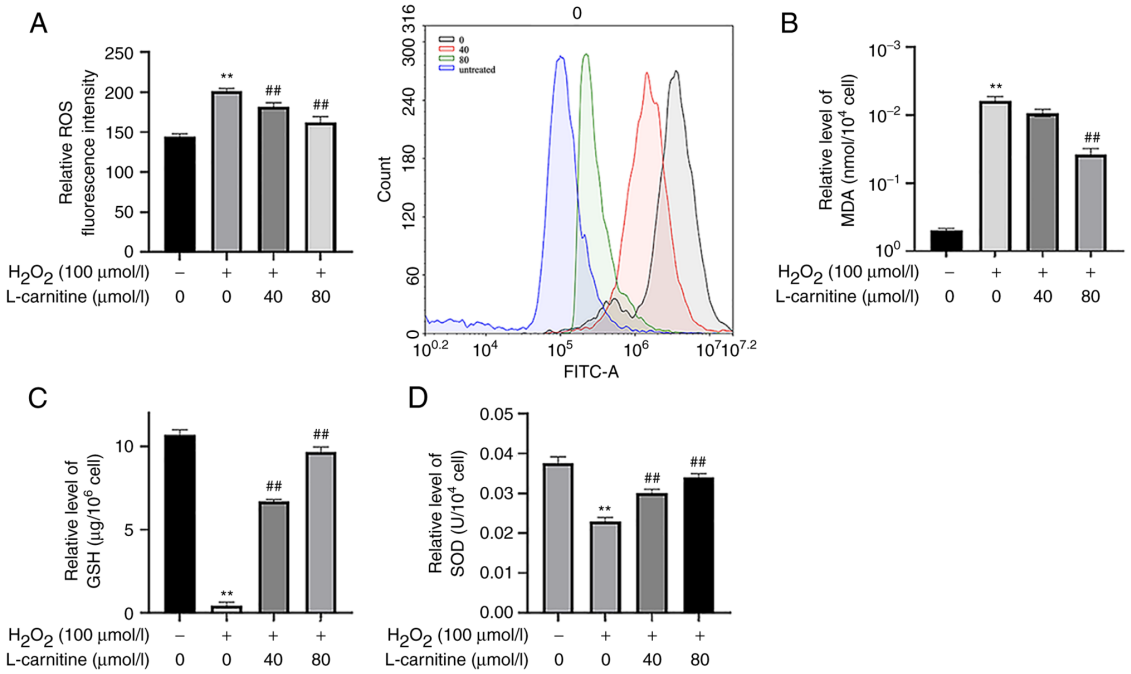

Figure 5. OS levels in KGN cells. (A) ROS content quantification and corresponding flow cytometry histogram. (B) MDA, (C) GSH and (D) SOD content. Compared with the control group, the KNG cells challenged with H_2O_2 showed an increase in the content of ROS and MDA, whilst the content of GSH and the activity of SOD were decreased. The OS injury model group was successfully constructed. Compared with that in the OS group, 40 and 80 μmol/l L-carnitine pre-treatment ameliorated the effect of H_2O_2 in KGN cells. **P<0.01 vs. untreated cells and $^{\#\#}$P<0.01 vs. H_2O_2-only; (A, C and D) Tukey's test; (B) Dunnett's T3 test. Data are presented as the mean ± standard deviation (n=3). OS, oxidative stress; ROS, reactive oxygen species; MDA, malondialdehyde; GSH, reduced glutathione; SOD, superoxide dismutase.

were visible under the light microscope, and aperture was visible around some cells, and the ability of cells to adhere to walls decreased. Under the electron microscope, the ultrastructural damage of cells was obvious, the intracellular apoptotic bodies increased, the nucleolus lobules increased, the nuclear membrane was blurred and unstructured, the mitochondria showed obvious swelling, and the mitochondrial crest fracture disappeared, showing early or late apoptotic manifestations. These characteristics include increased nucleolar lobulation, blurred nuclear membrane, mitochondrial swelling, mitochondrial cristae rupture and increased intracellular phagocytes.

OS biomarkers in KGN cells. After 100 μmol/l H_2O_2 induction, ROS and MDA levels in the H_2O_2-only group were significantly increased (P<0.01; Fig. 5A and B), whilst GSH content and SOD activity were significantly decreased compared with those in the control group (P<0.01; Fig. 5C and D). This suggest that 100 μmol/l H_2O_2 effectively induced OS injury in KGN cells. Compared with those in the H_2O_2-only group, the ROS and MDA levels in the 40 and 80 μmol/l LC pre-treatment groups were significantly decreased (P<0.05; Fig. 5A and B), whilst GSH content and SOD activity were significantly increased (P<0.01; Fig. 5C and D). In particular, the 80 μmol/l LC pre-treatment group exerted a greater effect compared with that by 40 μmol/l LC pre-treatment group.

ΔΨm and cell apoptosis of KGN cells. Compared with that in the control group, the ΔΨm in the H_2O_2-only group decreased significantly (P<0.01; Fig. 6A and B) whereas the

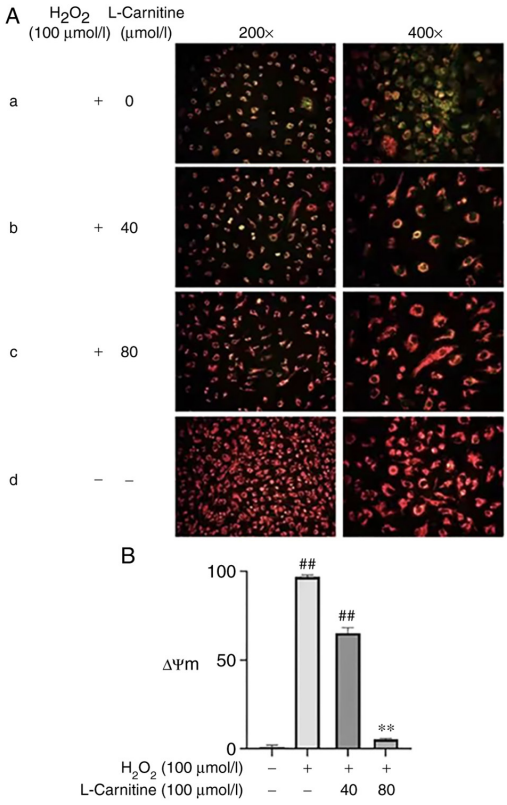

Figure 6. mitochondrial membrane potential of KGN cells. Mitochondrial membrane potential in the (A-a) H_2O_2-only, (A-b) low L-carnitine (40 μmol/l), (A-c) high L-carnitine (80 μmol/l) and (A-d) control groups. Magnification, x200. (B) Percentage of *ΔΨm* (JC-1 monomer-positive cells). **P<0.01 vs. control and $^{\#\#}$P<0.01 vs. H_2O_2-only, Tukey's test. Data are represented as the mean ± standard deviation (n=3).

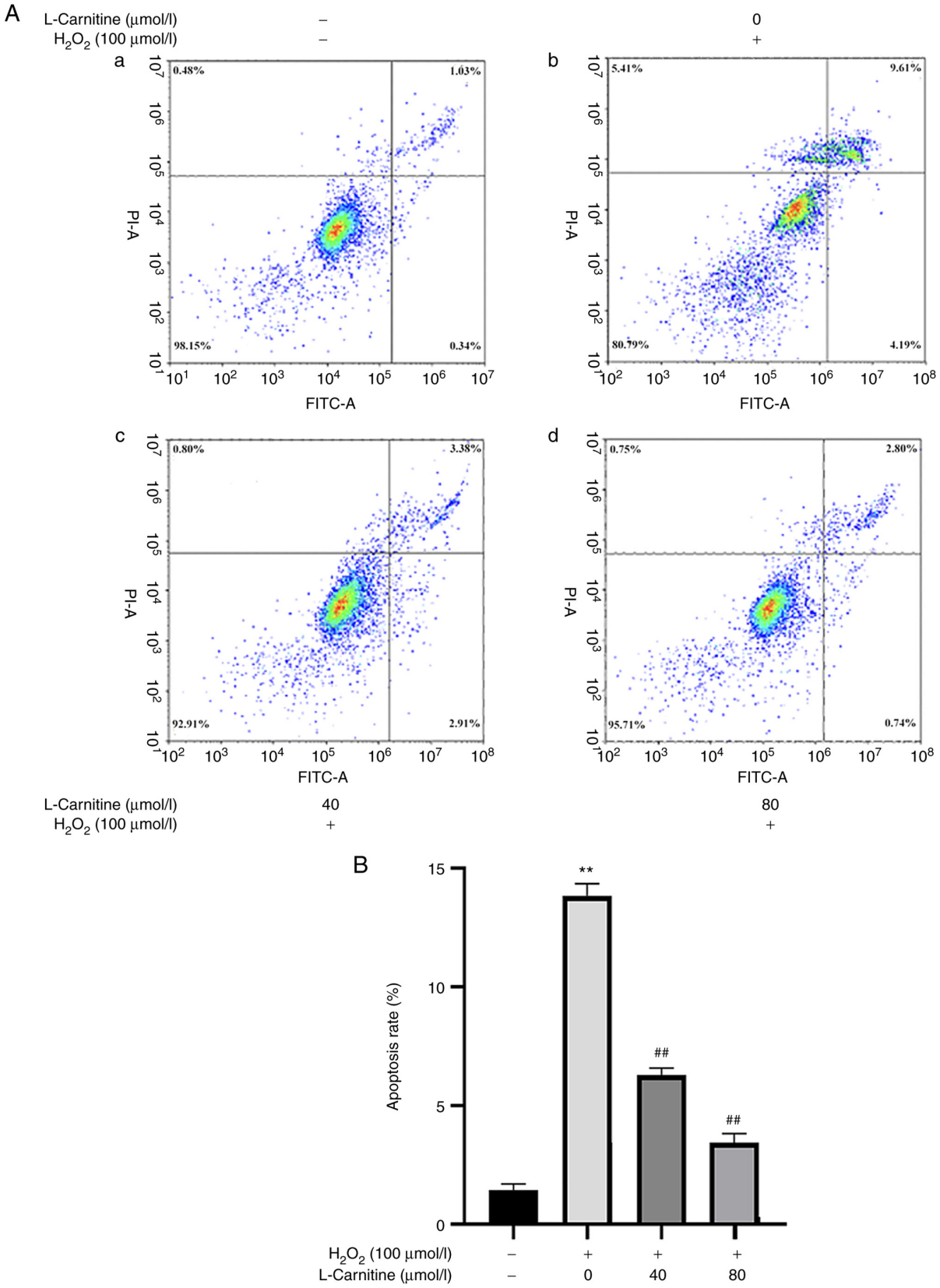

Figure 7. Cell apoptosis analysis through flow cytometry. (A) Representative flow cytometry dot plots in (A-a) H2O2-only, (A-b) low L-carnitine (40 μmol/l), (A-c) high L-carnitine (80 μmol/l) and (A-d) control groups (B) Percentage of apoptotic cells in each group. **P<0.01 vs. control and $^{\#\#}$P<0.01 vs. H_2O_2-only, Tukey's test. Data are represented as the mean ± standard deviation (n=3).

cell apoptosis rate was also significantly increased (P<0.01; Fig. 7A and B). Compared with those in the OS group, 40 and 80 μmol/l LC pre-treatment was able to significantly restore normal $\Delta\Psi$m (P<0.01; Fig. 6A and B) and significantly reduce the extent of cell apoptosis (P<0.01; Fig. 7A and B), with the effects mediated by 80 μmol/l LC being more potent. These

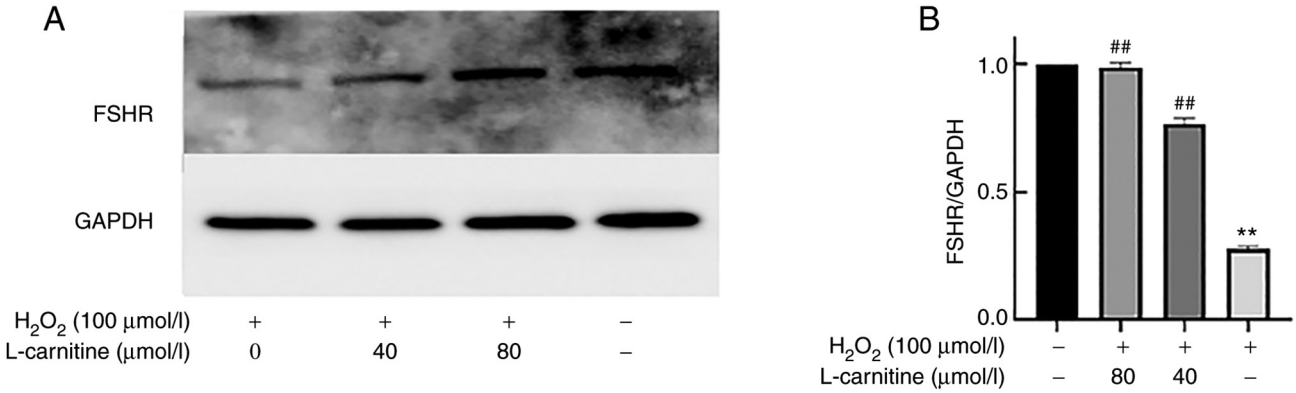

Figure 8. Effect of L-carnitine pretreatment on the expression of FSHR in KGN cells in a H_2O_2-induced oxidative stress injury model. (A) Representative western blotting image. (B) Densitometry data generated from the western blotting images. **P<0.01 vs. control and $^{\#\#}$P<0.01 vs. H_2O_2, Dunnett's T3 test. Data are represented as the mean ± standard deviation (n=3). FSHR, follicle stimulating hormone receptor.

results suggest that LC pretreatment can prevent the early apoptosis of KGN cells after OS injury and reduce the apoptosis rate after injury.

Expression level of the FSHR protein in KGN cells. Compared with that in the control group, the expression of FSHR in KGN cells was significantly decreased in the H_2O_2-only group (P<0.01; Fig. 8A and B). Compared with that in the H_2O_2-only group, 40 and 80 μmol/l LC pre-treatments could significantly increase FSHR protein expression (P<0.01; Fig. 8A and B).

Discussion

As one of the most important components of the follicle, ovarian GCs are involved in the mechanism of signal transduction and nutritional support to oocytes (18). The decrease in the number of GCs, as well as damage to their function, may lead to the decline of oocyte quality and eventually of ovarian function, which can cause female infertility (16).

The oocytes show different sensitivity to OS at different stages of follicle development (16). It is considered that once the dominant follicle enters the first stage of meiosis, a certain degree of OS is present to maintain high metabolic activity, whilst the subsequent process after of the first meiosis requires low OS to avoid cell damage (19). Compared with somatic cells, GCs have constitutively high metabolic levels during the entire process of follicular development, whilst the oxidation and antioxidant systems in the follicular microenvironment maintain a dynamic balance to meet the needs of the oocytes (15,16). When this system is disrupted by stress stimuli, OS and reduced local repair capability can change macromolecules, such as estradiol, production and induce mitochondrial mutations in the follicular microenvironment (20). A large number of follicle atresia causes an irreversible decline in ovarian function and eventually leads to premature ovarian failure (19). Previous studies have also found that the high level of ROS in the follicular fluid is associated with poor follicular quality, dysontogenesis and failure of *in vitro* fertilization-embryo transfer (IVF-ET) (19,21). In addition, the increase of ROS in the follicular fluid was also found in common female reproductive diseases, such as PCOS and EMT, suggesting that ROS may be associated with the occurrence and development of ovarian disorders (19). Therefore, it is important to protect ovarian GCs from OS damage for preserving female reproductive vitality.

LC is an amino acid analogue naturally occurring in the human body (13). It can promote lipid metabolism, protect plasma and mitochondrial membrane from damage by lipid peroxidation (19). LC has been widely used as an antioxidant (22), where it has been found that the addition of LC in sperm culture can improve sperm motility (22). In addition, LC treatment in the oocyte culture can improve oocyte quality, which may be associated with the reduction of GC apoptosis and improvement of mitochondrial function (23). It has also been reported that the administration of LC is beneficial to alleviate delayed embryonic development, DNA fragmentation and abnormal blastocyst development caused by long-term culture in elevated ROS conditions (24). Therefore, treatment with LC may have the potential to improve the quality of follicles and the pregnancy outcome following IVF-ET.

OS injury of GCs can lead to an imbalanced follicular microenvironment, reduced function of GCs and ovarian aging (24-26). The present study demonstrated that LC can effectively alleviate the generation of excess ROS induced by H_2O_2 by maintaining the redox balance. In addition, the level of MDA, the end-product of lipid peroxidation, was found to be significantly reduced in GCs after LC pre-treatment, suggesting that LC may alleviate the cell damage caused by OS and the mitochondrial oxidative respiratory chain. Analysis of SOD activity and GSH content revealed that LC pre-treatment may improve the antioxidant activity to reduce the consumption of antioxidants, which may in turn maintain the dynamic balance of redox species in the follicular microenvironment.

Damage of macromolecules, such as proteins and DNA, caused by OS eventually leads to the apoptosis of GCs (1). The present study showed that LC pre-treatment can effectively prevent the formation of apoptotic bodies, mitochondrial swelling and vacuolation, and nuclear membrane blurring induced by H_2O_2. The protective effects of LC was demonstrated by the fluorescence detection of $\Delta\Psi$m and cell apoptosis analysis. The expression of FSHR was higher in the cells with strong granulosa cell proliferation activity (27,28).

A previous study has suggested that OS can increase FSH activity by increasing the expression of P450 aromatase (9). Therefore, the present study aimed to use FSHR as an indicator to evaluate the function of GCs. The present results demonstrated that the expression level of FSHR in the H_2O_2-only group is significantly decreased compared with that in the control group. The expression of FSHR on GCs in the presence of H_2O_2 was significantly increased after pre-treatment with LC, further demonstrating the protective effect of LC. However, some limitations remain in the present study. The effect of LC on GCs has been investigated only *in vitro* since the number of granulosa cells collected could not meet the requirements of the experiment. In the future, it is important to build a rat model to confirm the effects of LC *in vivo*.

In conclusion, the present study suggest that LC treatment has the potential to reduce OS injury in GCs induced by H_2O_2 and decrease GC apoptosis. Therefore, LC may exert a protective effect on GCs, which could ensure improved nutritional support to oocytes and improve the quality of follicles.

Acknowledgements

Not applicable.

Funding

This work was supported by funding from Weifang Municipal Health Commission [grant number (wfwsjk_2019_029)].

Availability of data and materials

All data generated and/or analyzed during this study are included in this published article.

Authors' contributions

XL, XW and TM were responsible for designing the study, and analyzing and interpreting the data. XL performed the study in the laboratory in accordance with the methodology. XL and HM were responsible for the acquisition, analysis and interpretation of the data. HM and XL confirm the authenticity of all the raw data. XW, TM, YZ, PS and DQ provided scientific and technical assistance to the experiments, and critically revised the article for important intellectual content. XL collected samples and was responsible for the execution of the project. XL was responsible for the cellular and molecular experiments. All authors read and approved the final manuscript.

Ethics approval and consent to participate

Not applicable.

Patient consent for publication

Not applicable.

Competing interests

The authors declare that they have no competing interests.

References

1. Zhang J, Xu Y, Liu H and Pan Z: MicroRNAs in ovarian follicular atresia and granulosa cell apoptosis. Reprod Biol Endocrinol 17: 9, 2019.
2. Zhang H, Luo Q, Lu X, Yin N, Zhou D, Zhang L, Zhao W, Wang D, Du P, Hou Y, *et al*: Effects of hPMSCs on granulosa cell apoptosis and AMH expression and their role in the restoration of ovary function in premature ovarian failure mice. Stem Cell Res Ther 9: 20, 2018.
3. Matsuda F, Inoue N, Manabe N and Ohkura S: Follicular growth and atresia in mammalian ovaries: Regulation by survival and death of granulosa cells. J Reprod Dev 58: 44-50, 2012.
4. Terao H, Wada-Hiraike O, Nagumo A, Kunitomi C, Azhary JMK, Harada M, Hirata T, Hirota Y, Koga K, Fujii T and Osuga Y: Role of oxidative stress in follicular fluid on embryos of patients undergoing assisted reproductive technology treatment. J Obstet Gynaecol Res 45: 1884-1891, 2019.
5. Elmorsy E, Al-Ghafari A, Aggour AM, Khan R and Amer S: The role of oxidative stress in antipsychotics induced ovarian toxicity. Toxicol In Vitro 44: 190-195, 2017.
6. Lu J, Wang Z, Cao J, Chen Y and Dong Y: A novel and compact review on the role of oxidative stress in female reproduction. Reprod Biol Endocrinol 16: 80, 2018.
7. González F, Considine RV, Abdelhadi OA and Acton AJ: Oxidative stress in response to saturated fat ingestion is linked to insulin resistance and hyperandrogenism in polycystic ovary syndrome. J Clin Endocrinol Metab 104: 5360-5371, 2019.
8. Scutiero G, Iannone P, Bernardi G, Bonaccorsi G, Spadaro S, Volta CA, Greco P and Nappi L: Oxidative stress and endometriosis: A systematic review of the literature. Oxid Med Cell Longev 2017: 7265238, 2017.
9. Palumbo A, Rotoli D, Gonzalez-Fernandez R, Hernandez J and Avila J: Glucose-induced oxidative stress is associated with increased ALDH3A2 expression and altered response to FSH in cultured human granulosa-lutein cells (Gl cells) from young oocyte donors. Fertil Steril 100 (Suppl 1): S427, 2013.
10. González-Fernández R, Peña O, Hernández J, Martín-Vasallo P, Palumbo A and Avila J: FSH receptor, KL1/2, P450, and PAPP genes in granulosa-lutein cells from in vitro fertilization patients show a different expression pattern depending on the infertility diagnosis. Fertil Steril 94: 99-104, 2010.
11. Talenezhad N, Mohammadi M, Ramezani-Jolfaie N, Mozaffari-Khosravi H and Salehi-Abargouei A: Effects of l-carnitine supplementation on weight loss and body composition: A systematic review and meta-analysis of 37 randomized controlled clinical trials with dose-response analysis. Clin Nutr ESPEN 37: 9-23, 2020.
12. Carrillo-González DF, Hernández-Herrera DY and Maldonado-Estrada JG: The role of L-carnitine in bovine embryo metabolism. A review of the effect of supplementation with a metabolic modulator on in vitro embryo production. Anim Biotechnol: June 21, 2021 (Epub ahead of print).
13. Agarwal A, Sengupta P and Durairajanayagam D: Role of L-carnitine in female infertility. Reprod Biol Endocrinol 16: 5, 2018.
14. Li J, Liu L, Weng J, Yin TL, Yang J and Feng HL: Biological roles of l-carnitine in oocyte and early embryo development. Mol Reprod Dev 88: 673-685, 2021.
15. Nishi Y, Yanase T, Mu Y, Oba K, Ichino I, Saito M, Nomura M, Mukasa C, Okabe T, Goto K, *et al*: Establishment and characterization of a steroidogenic human granulosa-like tumor cell line, KGN, that expresses functional follicle-stimulating hormone receptor. Endocrinology 142: 437-445, 2001.
16. Tiwari M and Chaube SK: Moderate increase of reactive oxygen species triggers meiotic resumption in rat follicular oocytes. J Obstet Gynaecol Res 42: 536-546, 2016.
17. Ma B, Liu Y, Zhang X, Zhang R, Zhang Z, Zhang Z, Liu J, Juan Z, Sun X, Sun L, *et al*: TSPO ligands protect against neuronal damage mediated by LPS-induced BV-2 microglia activation. Oxid Med Cell Longev 2022: 5896699, 2022.
18. Silva EG, Kim G, Bakkar R, Bozdag Z, Shaye-Brown A, Loghavi S, Stolnicu S, Hadareanu V, Bulgaru D, Cayax LI, *et al*: Histology of the normal ovary in premenopausal patients. Ann Diagn Pathol 46: 151475, 2020.

19. Agarwal A, Aponte-Mellado A, Premkumar BJ, Shaman A and Gupta S: The effects of oxidative stress on female reproduction: A review. Reprod Biol Endocrinol 10: 49, 2012.
20. Prasad S, Tiwari M, Pandey AN, Shrivastav TG and Chaube SK: Impact of stress on oocyte quality and reproductive outcome. J Biomed Sci 23: 36, 2016.
21. Lee TH, Lee MS, Liu CH, Tsao HM, Huang CC and Yang YS: The association between microenvironmental reactive oxygen species and embryo development in assisted reproduction technology cycles. Reprod Sci 19: 725-732, 2012.
22. Fu LL, Zhang LY, An Q, Zhou F, Tong Y, Guo Y, Lu WH, Liang XW, Chang B and Gu YQ: L-carnitine protects the motion parameters and mitochondrial function of human sperm in cryopreservation. Zhonghua Nan Ke Xue 24: 1059-1063, 2018 (In Chinese).
23. Dunning KR, Russell DL and Robker RL: Lipids and oocyte developmental competence: The role of fatty acids and β-oxidation. Reproduction 148: R15-R27, 2014.
24. Kucukaydın Z, Duran C, Basaran M, Camlica F, Erdem SS, Basaran A, Kutlu O, Burnik FS, Elmas H and Gonen MS: Plasma total oxidant and antioxidant status after oral glucose tolerance and mixed meal tests in patients with polycystic ovary syndrome. J Endocrinol Invest 39: 1139-1148, 2016.
25. Yang L, Chen Y, Liu Y, Xing Y, Miao C, Zhao Y, Chang X and Zhang Q: The role of oxidative stress and natural antioxidants in ovarian aging. Front Pharmacol 11: 617843, 2021.
26. Peters AE, Mihalas BP, Bromfield EG, Roman SD, Nixon B and Sutherland JM: Autophagy in female fertility: A role in oxidative stress and aging. Antioxid Redox Signal 32: 550-568, 2020.
27. Yding Andersen C: Inhibin-B secretion and FSH isoform distribution may play an integral part of follicular selection in the natural menstrual cycle. Mol Hum Reprod 23: 16-24, 2017.
28. Knapczyk-Stwora K, Grzesiak M, Witek P, Duda M, Koziorowski M and Slomczynska M: Neonatal exposure to agonists and antagonists of sex steroid receptors affects AMH and FSH plasma level and their receptors expression in the adult pig ovary. Animals (Basel) 10: 12, 2019.